



This is a repository copy of *Erratum for the Report "A precise measurement of the magnetic field in the corona of the black hole binary V404 Cygni"*.

White Rose Research Online URL for this paper:
<http://eprints.whiterose.ac.uk/130317/>

Version: Accepted Version

Article:

Dallilar, Y., Eikenberry, S.S., Garner, A. et al. (64 more authors) (2018) Erratum for the Report "A precise measurement of the magnetic field in the corona of the black hole binary V404 Cygni". *Science*, 360 (6386). eaat9270. ISSN 0036-8075

<https://doi.org/10.1126/science.aat9270>

Reuse

Items deposited in White Rose Research Online are protected by copyright, with all rights reserved unless indicated otherwise. They may be downloaded and/or printed for private study, or other acts as permitted by national copyright laws. The publisher or other rights holders may allow further reproduction and re-use of the full text version. This is indicated by the licence information on the White Rose Research Online record for the item.

Takedown

If you consider content in White Rose Research Online to be in breach of UK law, please notify us by emailing eprints@whiterose.ac.uk including the URL of the record and the reason for the withdrawal request.



eprints@whiterose.ac.uk
<https://eprints.whiterose.ac.uk/>

Title: A Precise Measurement of the Magnetic Field in the Corona of the Black Hole Binary V404 Cygni

Authors: Yigit Dallilar^{1*}, Stephen S. Eikenberry^{1*}, Alan Garner¹, Richard D. Stelter¹, Amy Gottlieb¹, Poshak Gandhi², Piergiorgio Casella³, Vik S. Dhillon^{4,5}, Tom R. Marsh⁶, Stuart P. Littlefair⁴, Liam Hardy⁴, Rob Fender⁷, Kunal Mooley⁷, Dominic J. Walton⁸, Felix Fuerst^{9,10}, Matteo Bachetti¹¹, A.J. Castro-Tirado^{12,13}, Miguel Charcos¹, Michelle L. Edwards¹⁴, Nestor M. Lasso-Cabrera¹⁵, Antonio Marin-Franch¹⁵, S. Nicholas Raines¹, Kendall Ackley¹, John G. Bennett¹, A. Javier Cenarro¹⁵, Brian Chinn¹, H. Veronica Donoso¹, Raymond Frommeyer^{1†}, Kevin Hanna¹, Michael D. Herlevich¹, Jeff Julian¹, Paola Miller¹, Scott Mullin¹, Charles H. Murphey¹, Chris Packham^{16,17}, Frank Varosi¹, Claudia Vega¹, Craig Warner¹, A.N. Ramaprakash¹⁸, Mahesh Burse¹⁸, Sujit Punnadi¹⁸, Pravin Chordia¹⁸, Andreas Gerarts¹⁹, Héctor de Paz Martín¹⁹, María Martín Calero¹⁹, Riccardo Scarpa^{5,19}, Sergio Fernandez Acosta¹⁹, William Miguel Hernández Sánchez¹⁹, Benjamin Siegel¹⁹, Francisco Francisco Pérez¹⁹, Himar D. Viera Martín¹⁹, José A. Rodríguez Losada¹⁹, Agustín Nuñez¹⁹, Álvaro Tejero¹⁹, Carlos E. Martín González¹⁹, César Cabrera Rodríguez¹⁹, Jordi Molgó¹⁹, J. Esteban Rodríguez¹⁹, J. Israel Fernández Cáceres¹⁹, Luis A. Rodríguez García¹⁹, Manuel Huertas Lopez¹⁹, Raul Dominguez¹⁹, Tim Gaggstatter¹⁹, Antonio Cabrera Lavers¹⁹, Stefan Geier^{5,19}, Peter Pessev^{5,19}, Ata Sarajedini¹

Affiliations:

¹Department of Astronomy, University of Florida, 211 Bryant Space Science Center, Gainesville, FL 32611, USA.

²Department of Physics and Astronomy, University of Southampton, Highfield, Southampton SO17 1BJ, UK.

³Istituto Nazionale di Astrofisica - Osservatorio Astronomico di Roma, Via Frascati 33, I-00040 Monteporzio Catone, Italy.

⁴Department of Physics and Astronomy, University of Sheffield, Sheffield S3 7RH, UK.

⁵Instituto de Astrofisica de Canarias, 38205 La Laguna, Santa Cruz de Tenerife, Spain.

⁶Department of Physics, University of Warwick, Gibbet Hill Road, Coventry, CV4 7AL, UK.

⁷Division of Astrophysics, Department of Physics, University of Oxford, Keble Road, Oxford OX1 3RH, UK.

⁸Institute of Astronomy, University of Cambridge, Madingley Road, Cambridge CB3 0HA, UK.

⁹Space Radiation Laboratory, California Institute of Technology, Pasadena, CA 91125, USA.

¹⁰European Space Astronomy Centre, Operations Department, Villanueva de la Cañada, Madrid, Spain.

¹¹Istituto Nazionale di Astrofisica - Osservatorio Astronomico di Cagliari, via della Scienza 5, 09047 Selargius, Italy.

¹²Instituto de Astrofísica de Andalucía- Consejo Superior de Investigaciones Científicas, E-18008 Granada, Spain.

¹³Unidad Asociada Departamento de Ingeniería de Sistemas y Automática, Universidad de Málaga, 29071 Málaga, Spain.

¹⁴Large Binocular Telescope Observatory, University of Arizona, 933 North Cherry Avenue, Tucson, AZ 85721, USA.

¹⁵Centro de Estudios de Física del Cosmos de Aragón. 44001 Teruel, Aragón, Spain.

¹⁶Department of Physics and Astronomy. University of Texas at San Antonio. One UTSA Circle, San Antonio, TX 78249, USA.

¹⁷National Astronomical Observatory of Japan. 2-21-1 Osawa Mitaka Tokyo, 181-8588, Japan.

¹⁸Inter-University Center for Astronomy and Astrophysics, Post Bag 4, Ganeshkhind, Pune-411007, India.

¹⁹Gran Telescopio de Canarias, Cuesta de San José s/n, E-38712, Breña Baja, La Palma, Spain.

*Corresponding author. Email: ydallilar@ufl.edu (Y.D.); eiken@ufl.edu (S.S.E.)

†Deceased.

Abstract: Observations of binary stars containing an accreting black hole or neutron star often show x-ray emission extending to high energies (>10 kilo-electron volts), which is ascribed to an accretion disk corona of energetic particles akin to those seen in the solar corona. Despite their ubiquity, the physical conditions in accretion disk coronae remain poorly constrained. Using simultaneous infrared, optical, x-ray, and radio observations of the Galactic black hole system V404 Cygni, showing a rapid synchrotron cooling event in its 2015 outburst, we present a precise 33.1 ± 0.9 gauss magnetic field measurement in the corona of the Galactic black hole system V404 Cygni. This first high-precision measurement of the magnetic field in such a system is substantially lower than previous estimates for such systems, providing constraints on physical models of accretion physics in black hole and neutron star binary systems.

One Sentence Summary: We measure a magnetic field of 33.1 ± 0.9 gauss in the accretion disk corona of V404 Cygni - substantially lower than previous estimates and assumptions.

Main Text: Observations of accreting black hole systems reveal the existence of an accretion disk coronae (ADC) around the compact object – an energetic electron cloud primarily responsible for non-thermal emission. ADCs are thought to play a role in compact object accretion flows and energetics, especially in black hole binary systems that show relativistic jet outflows. Theoretical models predict that the thick geometry of an ADC leads to the magnetic field configuration required to power jet outflows, and spectral models show that the jet base is identical to the corona in these systems (1-3). However, we have few constraints on the detailed physical conditions in the jet-launching coronae.

The transient source V404 Cygni (Nova Cygni 1989) was discovered in 1989 (4), and subsequent observations revealed a black hole of 9 to 10 solar masses (M_{\odot}) in a 6.5-day binary orbit (5) with a $0.7 M_{\odot}$ companion star of spectral type K III; the system is located at a distance of 2.39 kpc (6). V404 Cyg produced an x-ray outburst starting on 15 June 2015 (7, 8) which lasted ~ 2 weeks. The outburst exhibited behavior including (i) complicated x-ray emission unlike the typical hard/soft states in black hole binaries, including occasional bright flares (9, 10); (ii) long-term correlations in the optical and x-ray lightcurves, attributed to thermal x-ray reprocessing (11); (iii) fast red optical flares lasting < 1 second, indicating optically thin synchrotron emission from compact regions probably located in a relativistic jet outflow (12);

(iv) variable polarization flares indicative of shocks propagating through a relativistic jet outflow (13) and (v) x-ray/radio correlations consistent with jet activity (14).

We present in Fig. 1 multiwavelength observations taken on 25 June 2015, 1 day after the jet-induced polarization flare observations (13) - in Fig. 1. These include near-infrared observations with the Canarias Infrared Camera Experiment (CIRCE) on the 10.4-meter Gran Telescopio Canarias (15), three-band optical observations with ULTRAFast CAMera (ULTRACAM) (12, 16) on the 4.2-meter William Herschel Telescope, x-ray observations from the Nuclear Spectroscopic Telescope Array (NuSTAR) satellite (17, 18), and three-band gigahertz radio observations with the Arcminute Microkelvin Imager (AMI) telescope (19). We dereddened the optical/infrared (OIR) data using an extinction estimate of $A_V = 4.0$ mag (6, 20). The radio, OIR, and x-ray bands exhibit quasi-independent behaviors. The infrared lightcurve resembles the optical lightcurves, including slow modulations of a few minutes with occasional fast flares [which match the jet-related fast flares seen the following day (12)]. The OIR flux levels are $>50\times$ higher than the quiescent flux from V404 Cygni as recorded in the Two Micron All Sky Survey (2MASS) catalog (21), indicating that the mass donor star contributes little light on this date, so the emission is dominated by outburst-related processes. The radio emission rises smoothly to 150 millijanskys (mJy) – an increase by a factor of ~ 10 over ~ 1 hr, also indicating jet activity (14). The complex x-ray lightcurve shows two episodes of enhanced x-ray activity coincident with slow modulations in the OIR lightcurves, as noted in previous studies of this outburst (9, 11). However, other slow OIR modulations exhibit no strong x-ray activity, indicating that the origin of the slow modulations must be more complex than a simple x-ray reprocessing scenario.

We focused on a selected time interval just before 57198.23 Modified Julian Date (MJD), at $t \sim 68$ minutes in Fig.1, when there was a sudden flux decay in all bands from infrared to x-ray. This decay came at the end of a ~ 30 -min episode of bright, slowly-varying OIR emission accompanied by several rapid x-ray flares. In 4 days of ULTRACAM observations of V404 Cygni around this outburst, this is the only such decay event, so it clearly differs from the rest of the observations [12, their figure 12]. We show this selected time interval in Fig. 2, with the OIR lightcurves normalized to pre-event fluxes. We modeled the flux profiles with an exponential decay function (Fig.2 and table S1). The characteristic timescale (τ) puts an upper limit on the size of the emitting region of $R < 1.25 c\tau$ via causality and time-of-flight arguments (20). This approach provides a firm upper limit to the ADC size; hence, considerably smaller values are possible.

To see whether a thermal blackbody could be the origin of the flux during this event, we took the observed color temperature from the ratio of g' and r' bands and calculated an expected thermal emission region size. The required thermal emission region is too large (more than a factor of 2) to match the observed variability timescale, and we can reject the thermally dominated emission hypothesis with a confidence $>5\sigma$ (fig. S1). This effectively eliminates blackbody emission processes [including X-ray reprocessing on the accretion disk or companion star (11)] as possible origins for the primary OIR emission during the event, and indicates that a nonthermal emission process (such as synchrotron or Compton scattering) must be the dominant source of the OIR flux. There is a small OIR flare at the top of the lightcurve just before the cooling event, which slightly lags the peak of the x-ray emission; this may be a low-amplitude x-ray reprocessing signature or an internal shock in a relativistic jet outflow (fig.S2).

The best fitting power-law function for $\tau(\nu)$ (table S1) is $\tau \propto \nu^{-0.49 \pm 0.03}$, where ν is the observed radiation frequency and τ represents the decay timescale in each band during the cooling

event in Fig. 2 (20). This result is consistent with the relation $\tau \propto \nu^{-1/2}$ characteristic of synchrotron cooling processes, which is more than five orders of magnitude in frequency (fig. 3). We eliminated Compton cooling as the origin of the cooling curve in the OIR band on the basis of magnetic to photon energy densities (20). Although we could not strictly eliminate Compton cooling for the x-rays, whereas we note that while thermal or Compton processes could possibly emulate this $\nu^{-1/2}$ frequency scaling, there is no a priori reason to expect them to do so, especially over such a large frequency range. This seems to confirm our conclusion that synchrotron processes dominate this event. Although x-ray measurements are consistent with our best fitting cooling curve within uncertainties, we observed flattening in the x-ray regime. Therefore, we cannot reject a possible contribution from Comptonization processes in the x-ray band (20).

We calculated individual synchrotron cooling magnetic field measurements from these timescales (table S1), obtaining a best-fitting mean magnetic field (B_0) of 33.1 ± 0.9 G, with reduced $\chi^2_\nu = 0.8$. The individual magnetic field values are all consistent with the mean value within their $\sim 1\sigma$ uncertainties (which are all 2 to 26%). Because a simple single-zone magnetic field model successfully fits all bands simultaneously, over 5 decades in energy for a time-coincident event, the dominant emission mechanism is consistent with a single population of electrons in a common magnetic field. The derived magnetic field has fractional uncertainties $25\times$ smaller than those in GX 339-04 (22). There is no apparent variation in the magnetic field strength during the event, from a decay timescale of <2 seconds in x-rays to >100 s in the OIR. We estimated a maximum fractional change in the magnetic field of $\Delta B/B_0 < 15\%$ (20). We could use this constraint to investigate possible expansion of the synchrotron-emitting region (because of expansion in a relativistic jet outflow). Magnetic field conservation arguments for adiabatically expanding synchrotron plasmoids generally lead to the conditions, $B \propto R^{-\alpha}$, where $1 < \alpha < 2$ and R is the radius of the synchrotron source (23). For the limiting case $\alpha = 1$, any fractional variation in the emitting region size is thus limited to $\Delta R/R < 15\%$. This upper limit suggests a stationary and stable region as the origin of the radiation: a stationary cloud of high-energy electrons confined to a small region. That is the expected disk corona structure for accreting black hole binaries, unlike discrete ejections expanding and moving at relativistic velocity (24).

Minimum energy requirements for synchrotron sources have been used to estimate equipartition magnetic field strengths in extragalactic and Galactic accreting black hole systems. Although there are some well-known caveats to this approach (25), recent studies have demonstrated evidence for charged-particle energies being in equilibrium with the magnetic field energy in a jet system (26). Applying these arguments to the V404 Cygni cooling event, we derive (20) an equipartition magnetic field strength B_{eq} of:

$$B_{eq} = 651 k^{2/7} (F_\nu/1 \text{ Jy})^{2/7} (\nu/10^{15} \text{ Hz})^{1/7} (\tau/2 \text{ sec})^{-6/7} \text{ Gauss, Equation 1}$$

where F_ν is the flux of the source at radiation frequency (ν) and k is defined to be the energy ratio of all charged particles to low-mass charged particles (electrons and positrons) in the system. We expect the k factor to be >1 for environments with relativistic bulk motions in which the mechanical energy of high-mass charged particles (protons or ions) dominates over the energy of low-mass charged particles. Because there is no clear evidence of bulk motions during the decay of the OIR flux, we assume $k \sim 1$. The derived equipartition field strength of ~ 650 G thus differs by a factor of **twenty** from the measured value of **33** G, indicating that

during this event V404 Cygni was **not in** an equipartition energy configuration. We can then derive the energetics in the system: the magnetic field energy $U_B = Vu_B \sim 4.0 \times 10^{34} (\tau/2 \text{ sec})^3$ ergs, electron kinetic energy $U_e = Vu_e \sim 1.1 \times 10^{39} (F_v/1 \text{ Jy})(\nu/10^{15} \text{ Hz})^{1/2}$ ergs, and the total energy $U_{\text{tot}} = U_B + U_e \sim 1.1 \times 10^{39}$ ergs (20). Here, V represents the emitting volume, and u_B and u_e are the magnetic field and electron energy densities respectively. During our observations, the OIR luminosities reach $\sim 10^{37}$ ergs/s, indicating that the overall energy stored in the corona is comparable to about **100 seconds** of the system's radiated energy, which is consistent with the rapid variations observed during this outburst being tied to and powered by variations in the accretion luminosity.

We present the overall spectral energy distribution (SED) at the start of the synchrotron cooling event in Fig.4, along with the corresponding electron energies and densities separately in fig. S3. The SED shown in the OIR regime is the excess flux with respect to the post-decay level [since thermal processes might be dominant in the remaining flux (20)]. The electron Lorentz factors γ range from $\gamma \sim 10$ for the radio to $\gamma \sim 10^3$ for the OIR bands and $\gamma \sim 10^5$ for the x-ray emission, covering the range from mildly relativistic to fully relativistic electrons. The overall distribution at the start of the event is the product of the history of relativistic electron injection into the coronal region at various times during the preceding activity in V404 Cygni, convolved with the relevant energy-dependent cooling timescales. We have no direct insight into the magnetic field properties during this time, nor into the acceleration mechanism populating the corona with relativistic electrons. However, if we assume that the cooling timescales (and thus magnetic field strengths) resemble those measured in the cooling event itself, we can infer possible scenarios. In particular, the x-ray cooling timescales (and associated x-ray emitting lifetimes of the electrons) would be very short (~ 2 seconds), so that the x-ray lightcurve variability would imply multiple electron acceleration/injection episodes over this period, each lasting several minutes and with substantial substructure. The observed correlation of the OIR flux with these events shows that the OIR variability is smoother – as expected for longer – timescale synchrotron cooling of lower-energy electrons. The observed correlations are not necessarily one-to-one between the OIR and x-rays, possibly implying a variable electron energy spectrum at the acceleration site.

Given the complex lightcurve history, multiple spectral breaks in the flux distribution (and inferred electron energy distribution) at the start of the fading event would arise naturally, as observed in Fig. 4 and fig. S3. For example, the x-ray spectral/energy distribution does not connect smoothly with the OIR region. Again, this is consistent with the much shorter synchrotron timescale for the x-ray emitting electrons (and thus shorter effective memory of the system), compared with the typical time between injection episodes of 10 to 100s, which are comparable with or shorter than the expected OIR synchrotron cooling timescales. There is another spectral break between the OIR and radio emission, as commonly seen in black hole binaries, and usually interpreted as increasing self-absorbed synchrotron emission from a radio photosphere with radius $\sim 10^{12}$ to 10^{13} cm (20) containing low-energy electrons. The corresponding light-crossing times are hundreds of seconds, and the presence of a radio photosphere is possibly tied to a large-scale jet feature. This matches both the observed smoothness of the radio lightcurve and the expected synchrotron opacity at these electron energies/densities for the measured field strength. The OIR emission is expected to be optically thin, and thus on the other side of this opacity-induced break.

Our magnetic field measurement provides constraints on jet launching or emission models, especially because it is much lower than previous estimates for other sources: $\sim 10^5$ - 10^7 G for Cyg X-1 (27), $\sim 5 \times 10^4$ G for XTE J1550-564 (28), and $1.5(\pm 0.8) \times 10^4$ G for GX 339-04 (21). A lower field requires an electron energy distribution with higher Lorentz factors (by a factor of 30 or more). Assuming equipartition configuration, it also implies a larger size for the emitting region ($R \propto B_{eq}^{-7/6}$) (Eq. 1) and lower particle density ($n_e \propto B_{eq}^{5/2}$) (20). Previous studies have followed a scaling relation between inferred magnetic field and spectral break frequency ν_b in the SED of $B \sim \nu_b L^{-1/9}$ (28, 29). If we associate the OIR peak in Fig. 4 with this break and scale from GX 339-04, we would expect $B \sim 2 \times 10^5$ G for V404 Cygni – which is too high by a factor of ~ 6000 – indicating that the scaling relation may not hold as broadly or simply as previously thought. However, the decay event here only reveals the physical conditions in the jet-launching corona at the time when electron injection/acceleration stops. We have no direct information regarding the process that accelerates the electron population in the first place. A non-expanding emission region that is physically distinct from the acceleration region in V404 Cygni (and not previously seen in the other sources) could also explain the scaling difference, albeit while requiring that jet base structure varies between sources.

References and Notes:

1. D. L. Meier, The association of jet production with geometrically thick accretion flows and black hole rotation. *Astrophys. J.* **548**, L9–L12 (2001).
2. S. Markoff, H. Falcke, R. Fender, A jet model for the broadband spectrum of XTE J1118+480. Synchrotron emission from radio to x-rays in the low/hard spectral state. *Astron. Astrophys.* **372**, L25–L28 (2001).
3. S. Markoff, M. Nowak, S. Corbel, R. Fender, H. Falcke, Exploring the role of jets in the radio/x-ray correlations of GX 339-4. *Astron. Astrophys.* **397**, 645–658 (2003).
4. F. Makino, GS 2023+338. *Int. Astron. Union Circ. no. 4782*, B. G. Marsden, Ed. (1989).
5. J. Casares, P. A. Charles, D. H. P. Jones, R. G. M. Rutten, P. J. Callanan, Optical studies of V404 Cyg, the x-ray transient GS2023+338. I. The 1989 outburst and decline. *Mon. Not. R. Astron. Soc.* **250**, 712–725 (1991).
6. J. C. A. Miller-Jones, P. G. Jonker, V. Dhawan, W. Briskin, M. P. Rupen, G. Nelemans, E. Gallo, The first accurate parallax distance to a black hole. *Astrophys. J.* **706**, L230–L234 (2009).
7. S. D. Barthelmy, A. D’ai, P. D’Avanzo, Swift trigger 643949 is V404 Cyg. *The Gamma-ray Coordinates Network Circ. no. 17929* (2015).
8. H. Negoro et al., MAXI/GSC detection of a new outburst from the Galactic black hole candidate GS 2023+338 (V* V404 Cyg). *The Astronomer’s Telegram. no. 7646* (2015).
9. J. Rodriguez, M. Cadolle Bel, J. Alfonso-Garzón, T. Siegert, X.-L. Zhang, V. Grinberg, V. Savchenko, J. A. Tomsick, J. Chenevez, M. Clavel, S. Corbel, R. Diehl, A. Domingo, C.

Gouiffès, J. Greiner, M. G. H. Krause, P. Laurent, A. Loh, S. Markoff, J. M. Mas-Hesse, J. C. A. Miller-Jones, D. M. Russell, J. Wilms, Correlated optical, x-ray, and γ -ray flaring activity seen with INTEGRAL during the 2015 outburst of V404 Cygni. *Astron. Astrophys.* **581**, L9 (2015).

10. T. M. Belloni, “States and transitions in black hole binaries” in *The Jet Paradigm: From Microquasars to Quasars* (Springer-Verlag, 2010).

11. M. Kimura, K. Isogai, T. Kato, Y. Ueda, S. Nakahira, M. Shidatsu, T. Enoto, T. Hori, D. Nogami, C. Littlefield, R. Ishioka, Y.-T. Chen, S.-K. King, C.-Y. Wen, S.-Y. Wang, M. J. Lehner, M. E. Schwamb, J.-H. Wang, Z.-W. Zhang, C. Alcock, T. Axelrod, F. B. Bianco, Y.-I. Byun, W.-P. Chen, K. H. Cook, D.-W. Kim, T. Lee, S. L. Marshall, E. P. Pavlenko, O. I. Antonyuk, K. A. Antonyuk, N. V. Pit, A. A. Sosnovskij, J. V. Babina, A. V. Baklanov, A. S. Pozanenko, E. D. Mazaeva, S. E. Schmalz, I. V. Reva, S. P. Belan, R. Y. Inasaridze, N. Tungalag, A. A. Volnova, I. E. Molotov, E. de Miguel, K. Kasai, W. L. Stein, P. A. Dubovsky, S. Kiyota, I. Miller, M. Richmond, W. Goff, M. V. Andreev, H. Takahashi, N. Kojiguchi, Y. Sugiura, N. Takeda, E. Yamada, K. Matsumoto, N. James, R. D. Pickard, T. Tordai, Y. Maeda, J. Ruiz, A. Miyashita, L. M. Cook, A. Imada, M. Uemura, Repetitive patterns in rapid optical variations in the nearby black-hole binary V404 Cygni. *Nature* **529**, 54–58 (2016).

12. P. Gandhi, S. P. Littlefair, L. K. Hardy, V. S. Dhillon, T. R. Marsh, A. W. Shaw, D. Altamirano, M. D. Caballero-Garcia, J. Casares, P. Casella, A. J. Castro-Tirado, P. A. Charles, Y. Dallilar, S. Eikenberry, R. P. Fender, R. I. Hynes, C. Knigge, E. Kuulkers, K. Mooley, T. Muñoz-Darias, M. Pahari, F. Rahoui, D. M. Russell, J. V. Hernández Santisteban, T. Shahbaz, D. M. Terndrup, J. Tomsick, D. J. Walton, Furiously fast and red: Sub-second optical flaring in V404 Cyg during the 2015 outburst peak. *Mon. Not. R. Astron. Soc.* **459**, 554–572 (2016).

13. T. Shahbaz, D. M. Russell, S. Covino, K. Mooley, R. P. Fender, C. Rumsey, Evidence for magnetic field compression in shocks within the jet of V404 Cyg. *Mon. Not. R. Astron. Soc.* **463**, 1822–1830 (2016).

14. R. M. Plotkin, J. C. A. Miller-Jones, E. Gallo, P. G. Jonker, J. Homan, J. A. Tomsick, P. Kaaret, D. M. Russell, S. Heinz, E. J. Hodges-Kluck, S. Markoff, G. R. Sivakoff, D. Altamirano, J. Nielsen, The 2015 decay of the black hole x-ray binary V404 Cygni: Robust disk-jet coupling and a sharp transition into quiescence. *Astrophys. J.* **834**, 104 (2017).

15. S. S. Eikenberry et al., arXiv:1709.05542 [astro-ph.IM] (2017).

16. V. S. Dhillon, T. R. Marsh, M. J. Stevenson, D. C. Atkinson, P. Kerry, P. T. Peacocke, A. J. A. Vick, S. M. Beard, D. J. Ives, D. W. Lunney, S. A. McLay, C. J. Tierney, J. Kelly, S. P. Littlefair, R. Nicholson, R. Pashley, E. T. Harlaftis, K. O’Brien, ULTRACAM: An ultrafast, triple-beam CCD camera for high-speed astrophysics. *Mon. Not. R. Astron. Soc.* **378**, 825–840 (2007).

17. F. A. Harrison, W. W. Craig, F. E. Christensen, C. J. Hailey, W. W. Zhang, S. E. Boggs, D. Stern, W. R. Cook, K. Forster, P. Giommi, B. W. Grefenstette, Y. Kim, T. Kitaguchi, J. E. Koglin, K. K. Madsen, P. H. Mao, H. Miyasaka, K. Mori, M. Perri, M. J. Pivovarov, S. Puccetti,

- V. R. Rana, N. J. Westergaard, J. Willis, A. Zoglauer, H. An, M. Bachetti, N. M. Barrière, E. C. Bellm, V. Bhalerao, N. F. Brejnholt, F. Fuerst, C. C. Liebe, C. B. Markwardt, M. Nynka, J. K. Vogel, D. J. Walton, D. R. Wik, D. M. Alexander, L. R. Cominsky, A. E. Hornschemeier, A. Hornstrup, V. M. Kaspi, G. M. Madejski, G. Matt, S. Molendi, D. M. Smith, J. A. Tomsick, M. Ajello, D. R. Ballantyne, M. Baloković, D. Barret, F. E. Bauer, R. D. Blandford, W. N. Brandt, L. W. Brenneman, J. Chiang, D. Chakrabarty, J. Chenevez, A. Comastri, F. Dufour, M. Elvis, A. C. Fabian, D. Farrah, C. L. Fryer, E. V. Gotthelf, J. E. Grindlay, D. J. Helfand, R. Krivonos, D. L. Meier, J. M. Miller, L. Natalucci, P. Ogle, E. O. Ofek, A. Ptak, S. P. Reynolds, J. R. Rigby, G. Tagliaferri, S. E. Thorsett, E. Treister, C. M. Urry, The Nuclear Spectroscopic Telescope Array (NuSTAR) high-energy x-ray mission. *Astrophys. J.* **770**, 103 (2013).
18. D. Walton, K. Mooley, A. L. King, J. A. Tomsick, J. M. Miller, T. Dauser, J. A. García, M. Bachetti, M. Brightman, A. C. Fabian, K. Forster, F. Fürst, P. Gandhi, B. W. Grefenstette, F. A. Harrison, K. K. Madsen, D. L. Meier, M. J. Middleton, L. Natalucci, F. Rahoui, V. Rana, D. Stern, Living on a flare: Relativistic reflection in V404 Cyg observed by NuSTAR during its summer 2015 outburst. *Astrophys. J.* **839**, 110 (2017).
19. J. T. L. Zwart, R. W. Barker, P. Biddulph, D. Bly, R. C. Boyesen, A. R. Brown, C. Clementson, M. Crofts, T. L. Culverhouse, J. Czeres, R. J. Dace, M. L. Davies, R. D’Alessandro, P. Doherty, K. Duggan, J. A. Ely, M. Felvus, F. Feroz, W. Flynn, T. M. O. Franzen, J. Geisbüsch, R. Génova-Santos, K. J. B. Grainge, W. F. Grainger, D. Hammett, R. E. Hills, M. P. Hobson, C. M. Holler, N. Hurley-Walker, R. Jilley, M. E. Jones, T. Kaneko, R. Kneissl, K. Lancaster, A. N. Lasenby, P. J. Marshall, F. Newton, O. Norris, I. Northrop, D. M. Odell, G. Petencin, J. C. Pober, G. G. Pooley, M. W. Pospieszalski, V. Quy, C. Rodríguez-Gonzálvez, R. D. E. Saunders, A. M. M. Scaife, J. Schofield, P. F. Scott, C. Shaw, T. W. Shimwell, H. Smith, A. C. Taylor, D. J. Titterton, M. Velić, E. M. Waldram, S. West, B. A. Wood, G. Yassin, The arcminute microkelvin imager. *Mon. Not. R. Astron. Soc.* **391**, 1545–1558 (2008).
20. Materials and methods are available as supplementary materials.
21. R. M. Cutri et al., 2MASS all-sky catalog of point sources. VizieR Online Data Catalog. no. 2246 (2003).
22. P. Gandhi, A. W. Blain, D. M. Russell, P. Casella, J. Malzac, S. Corbel, P. D’Avanzo, F. W. Lewis, S. Markoff, M. Cadolle Bel, P. Goldoni, S. Wachter, D. Khangulyan, A. Mainzer, A variable mid-infrared synchrotron break associated with the compact jet in GX 339-4. *Astrophys. J.* **740**, L13 (2011).
23. H. C. Spruit, F. Daigne, G. Drenkhahn, Large scale magnetic fields and their dissipation in GRB fireballs. *Astron. Astrophys.* **369**, 694–705 (2001).
24. R. Fender, “‘Disc-Jet’ coupling in black hole X-ray binaries and active galactic nuclei,” in *The Jet Paradigm: From Microquasars to Quasars* (Springer-Verlag, 2010).
25. A. A. Zdziarski, The minimum jet power and equipartition. *Mon. Not. R. Astron. Soc.* **445**, 1321–1330 (2014).

26. L. Stawarz, Y. T. Tanaka, G. Madejski, S. P. O’Sullivan, C. C. Cheung, I. J. Feain, Y. Fukazawa, P. Gandhi, M. J. Hardcastle, J. Kataoka, M. Ostrowski, B. Reville, A. Siemiginowska, A. Simionescu, T. Takahashi, Y. Takei, Y. Takeuchi, N. Werner, Giant lobes of Centaurus A radio galaxy observed with the Suzaku x-ray satellite. *Astrophys. J.* **766**, 48 (2013).
27. M. Del Santo, J. Malzac, R. Belmont, L. Bouchet, G. De Cesare, The magnetic field in the X-ray corona of Cygnus X-1. *Mon. Not. R. Astron. Soc.* **430**, 209–220 (2013).
28. S. Chaty, G. Dubus, A. Raichoor, Near-infrared jet emission in the microquasar XTE J1550-564. *Astron. Astrophys.* **529**, A3 (2011).
29. D. M. Russell, S. Markoff, P. Casella, A. G. Cantrell, R. Chatterjee, R. P. Fender, E. Gallo, P. Gandhi, J. Homan, D. Maitra, J. C. A. Miller-Jones, K. O’Brien, T. Shahbaz, Jet spectral breaks in black hole x-ray binaries. *Mon. Not. R. Astron. Soc.* **429**, 815–832 (2013).
30. N. Zacharias, C. Finch, J. Subasavage, G. Bredthauer, C. Crockett, M. Divittorio, E. Ferguson, F. Harris, H. Harris, A. Henden, C. Kilian, J. Munn, T. Rafferty, A. Rhodes, M. Schultheiss, T. Tilleman, G. Wieder, The first U.S. Naval Observatory Robotic Astrometric Telescope Catalog. *Astron. J.* **150**, 101 (2015).
31. 4 PI SKY. Exploring the Transient Universe: <https://4pisky.org/>
32. M. L. Davies, T. M. O. Franzen, R. D. Davies, R. J. Davis, F. Feroz, R. Génova-Santos, K. J. B. Grainge, D. A. Green, M. P. Hobson, N. Hurley-Walker, A. N. Lasenby, M. López-Cañiego, M. Olamaie, C. P. Padilla-Torres, G. G. Pooley, R. Rebolo, C. Rodríguez-González, R. D. E. Saunders, A. M. M. Scaife, P. F. Scott, T. W. Shimwell, D. J. Titterton, E. M. Waldram, R. A. Watson, J. T. L. Zwart, Follow-up observations at 16 and 33-GHz of extragalactic sources from WMAP 3-yr data: I—Spectral properties. *Mon. Not. R. Astron. Soc.* **400**, 984–994 (2009).
33. Y. C. Perrott, A. M. M. Scaife, D. A. Green, M. L. Davies, T. M. O. Franzen, K. J. B. Grainge, M. P. Hobson, N. Hurley-Walker, A. N. Lasenby, M. Olamaie, G. G. Pooley, C. Rodríguez-González, C. Rumsey, R. D. E. Saunders, M. P. Schammel, P. F. Scott, T. W. Shimwell, D. J. Titterton, E. M. Waldram, AMI Galactic Plane Survey at 16 GHz - I. Observing, mapping and source extraction. *Mon. Not. R. Astron. Soc.* **429**, 3330–3340 (2013).
34. J. P. McMullin, B. Waters, D. Schiebel, W. Young, K. Golap, *Astronomical Data Analysis Software and Systems XVI*, Astronomical Society of the Pacific Conference Series, San Francisco, California, R. A. Shaw, F. Hill, D. J. Bell, Eds. (2007), vol. 376.
35. M. Bachetti, F. A. Harrison, R. Cook, J. Tomsick, C. Schmid, B. W. Grefenstette, D. Barret, S. E. Boggs, F. E. Christensen, W. W. Craig, A. C. Fabian, F. Fürst, P. Gandhi, C. J. Hailey, E. Kara, T. J. Maccarone, J. M. Miller, K. Pottschmidt, D. Stern, P. Uttley, D. J. Walton, J. Wilms, W. W. Zhang, No time for deadline: Timing analysis of bright black hole binaries with NuSTAR. *Astrophys. J.* **800**, 109 (2015).

36. K. K. Madsen, S. Reynolds, F. Harrison, H. An, S. Boggs, F. E. Christensen, W. W. Craig, C. L. Fryer, B. W. Grefenstette, C. J. Hailey, C. Markwardt, M. Nynka, D. Stern, A. Zoglauer, W. Zhang, Broadband x-ray imaging and spectroscopy of the Crab Nebula and Pulsar with NuSTAR. *Astrophys. J.* **801**, 66 (2015).
37. M. Bachetti, MaLTPyNT: Quick look timing analysis for NuSTAR data. Astrophysics Source Code Library. no. 02021B (2015).
38. D. J. Schlegel, D. P. Finkbeiner, M. Davis, Maps of dust infrared emission for use in estimation of reddening and cosmic microwave background radiation foregrounds. *Astrophys. J.* **500**, 525–553 (1998).
39. S. S. Eikenberry, K. Matthews, E. H. Morgan, R. A. Remillard, R. W. Nelson, Evidence for a disk-jet interaction in the microquasar GRS 1915+105. *Astrophys. J.* **494**, L61–L64 (1998).
40. Z. L. Uhm, B. Zhang, Fast-cooling synchrotron radiation in a decaying magnetic field and gamma-ray burst emission mechanism. *Nat. Phys.* **10**, 351–356 (2014).
41. M. S. Longair, *High Energy Astrophysics*. (Cambridge Univ. Press, ed. 3, 2011).
42. A. K. Kembhavi, J. V. Narlikar, *Quasars and Active Galactic Nuclei: An Introduction*. (Cambridge University Press, 1999).

Acknowledgements: The near-infrared lightcurve is based on observations made with the Gran Telescopio Canarias, installed in the Spanish Observatorio del Roque de los Muchachos of the Instituto de Astrofísica de Canarias, in the island of La Palma, during science commissioning of CIRCE. Development of CIRCE was supported by the University of Florida and the National Science Foundation (grant AST-0352664), in collaboration with Inter-University Centre for Astronomy and Astrophysics. The William Herschel Telescope is operated on the island of La Palma by the Isaac Newton Group in the Spanish Observatorio del Roque de los Muchachos of the Instituto de Astrofísica de Canarias. The ULTRACAM team and PG (grant ST/J003697/2) acknowledge the financial support of the UK Science and Technology Facilities Council. This research has made use of data obtained with NuSTAR, a project led by the California Institute of Technology, funded by NASA and managed by NASA/Jet Propulsion Laboratory, and has used the NUSTARDAS software package, jointly developed by the Agenzia Spaziale Italiana Science Data Center (Italy) and Caltech (USA). AJCT acknowledges support from the Spanish Ministry Project AYA2015-71718-R. We thank S. Markoff, C. Ceccobello, and T. Maccarone for comments on the scientific discussion. The multi-wavelength lightcurves are provided as data file S1 and our derived measurements are listed in table S1. The observational data are available for each instrument: CIRCE at <http://astro.ufl.edu/~ydallilar/Dallilar17/CIRCEraw> ; ULTRACAM at https://sotonac-my.sharepoint.com/personal/pg3e14_soton_ac_uk/Documents/Forms/All.aspx?slrid=603d299e%2D704d%2D4000%2Ddbf01%2Dc1708c50f62d&RootFolder=%2Fpersonal%2Fpg3e14%5Fsoton%5Fac%5Fuk%2FDocuments%2Fv404&FolderCTID=0x012000F83BE7EA86B4FE49BECFDAA6CEB2B068 (in ULTRACAM pipeline binary format); NuSTAR at <https://heasarc.gsfc.nasa.gov/FTP/nustar/data/obs/01/9/90102007011>; and AMI at http://www.tauceti.caltech.edu/kunal/uploads/SWIFT_643949-150625.fits (in radio Flexible Image Transport System format).

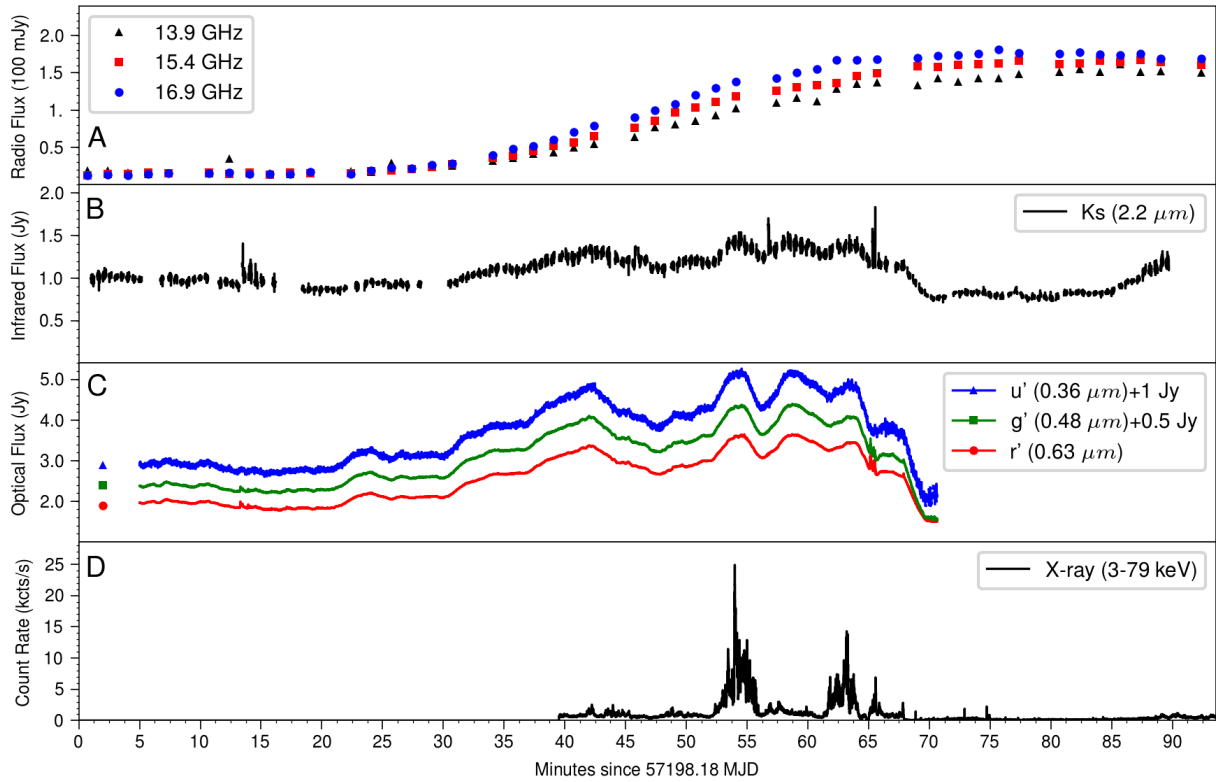


Fig. 1. Multi-wavelength light curves of V404 Cygni on MJD 57198 during the 2015 outburst. (A to D) Observational light curves are shown for (A) three radio frequencies, (B) the infrared Ks band, (C) the r' , g' and u' optical bands, and (D) 3 to 79 keV x-rays. The optical and infrared bands show slow modulations punctuated by fast red flares. The two optical bumps at ~ 54 and ~ 63 minutes coincide with bright x-ray flares, whereas the bumps at ~ 42 and ~ 58 minutes shows very little (if any) X-ray activity, indicating that models invoking simple X-ray reprocessing cannot reproduce the multi-wavelength light curve. The cooling event is at ~ 68 minutes.

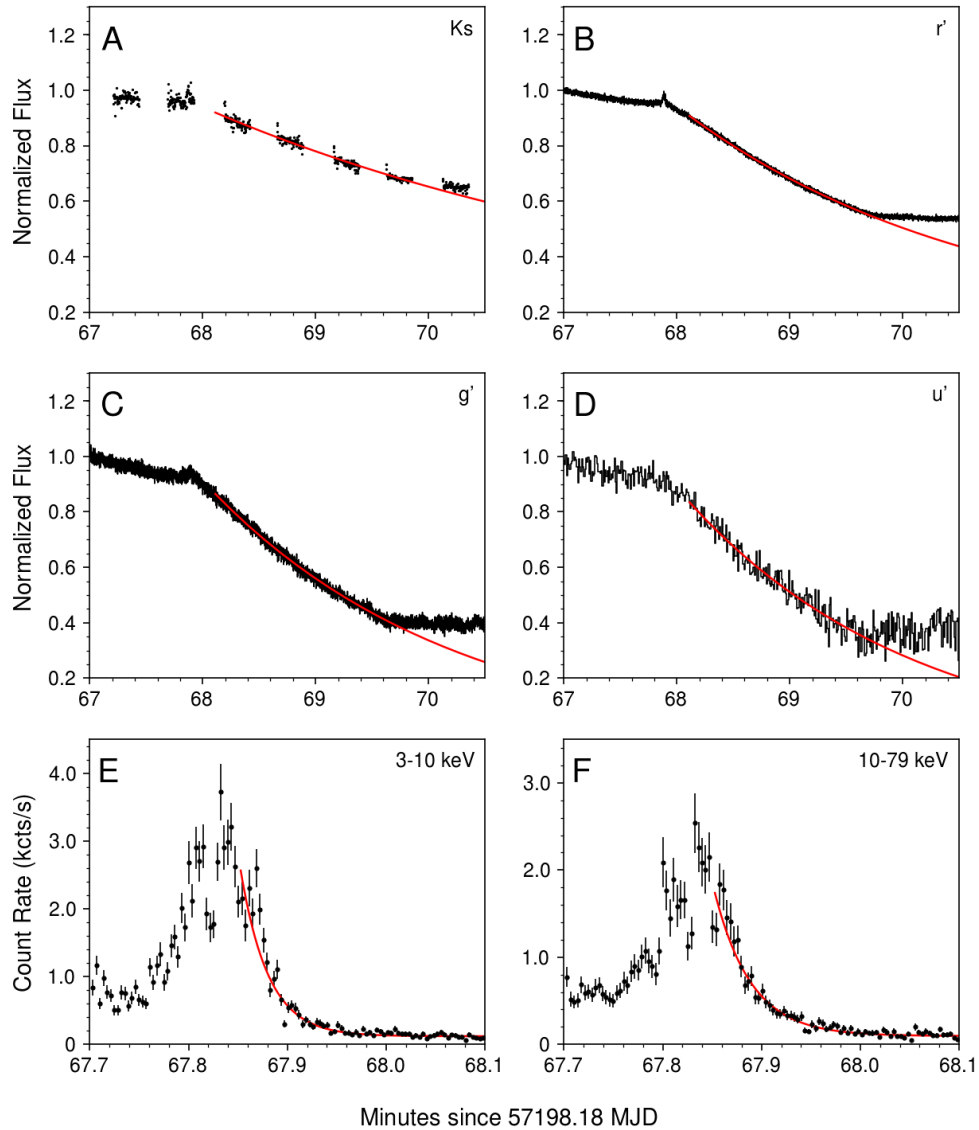


Fig. 2. Simultaneous cooling event decay curves with best-fit exponential models. (A to F) Black lines represent the data, and red lines indicate the best-fit exponential decay profile for the six different energy bands: (A) infrared Ks band; (B), (C), (D), optical r' , g' , u' bands; and (E) and (F), x-ray 3-10 keV and 10-79 keV. The measured timescales for each are given in table S1.

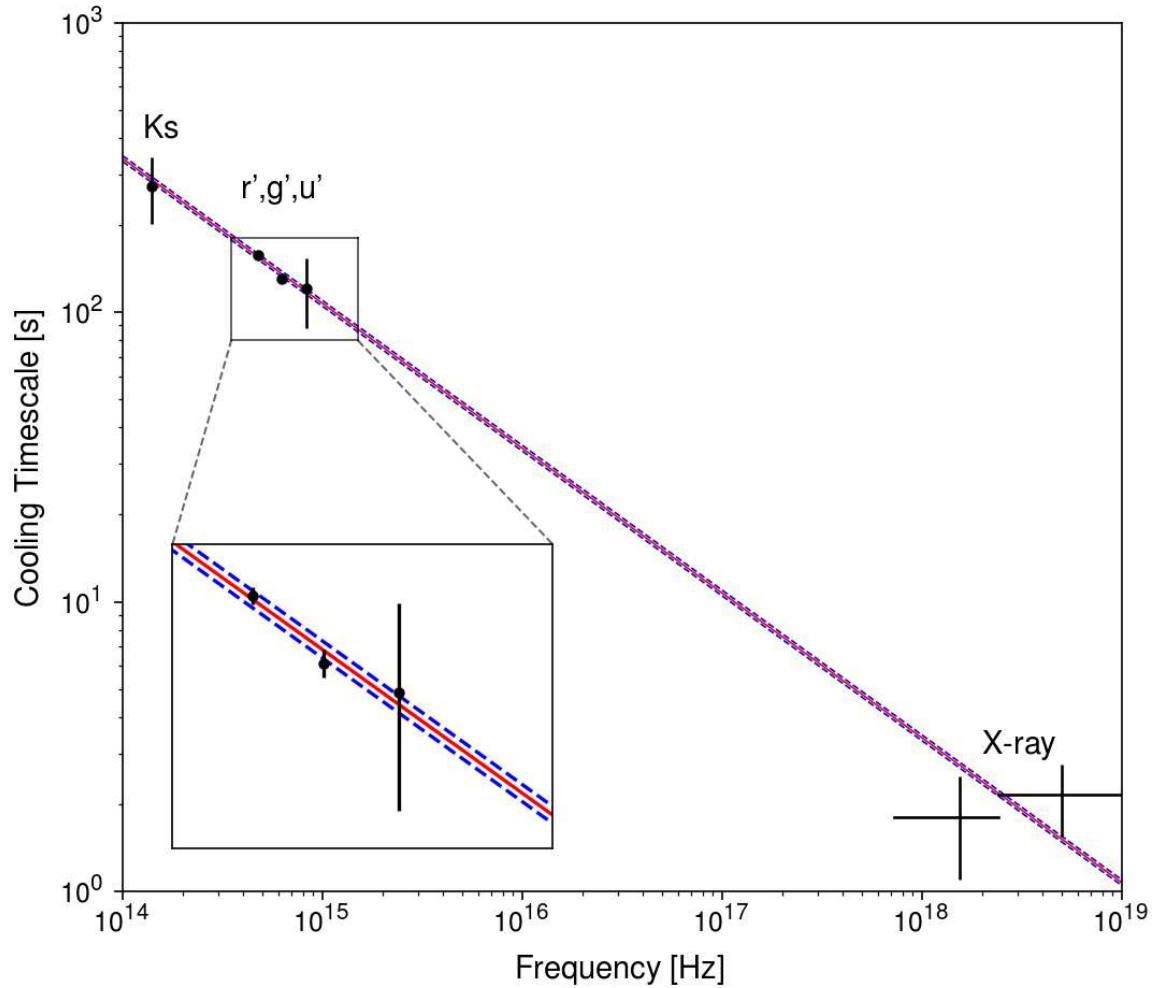


Fig. 3. Cooling timescales as a function of observed radiation frequencies from near-infrared to x-rays. The solid red line shows the best-fitting single-zone magnetic field strength of **33.1 G**, with dashed lines at ± 0.9 G uncertainty. The model is fitted over 5 orders of magnitude in frequency; it has a reduced $\chi^2_{\nu} = 0.8$ and a power-law dependence of $\tau \sim \nu^{-0.49 \pm 0.03}$, which is consistent with the $\nu^{-1/2}$ expected for synchrotron cooling.

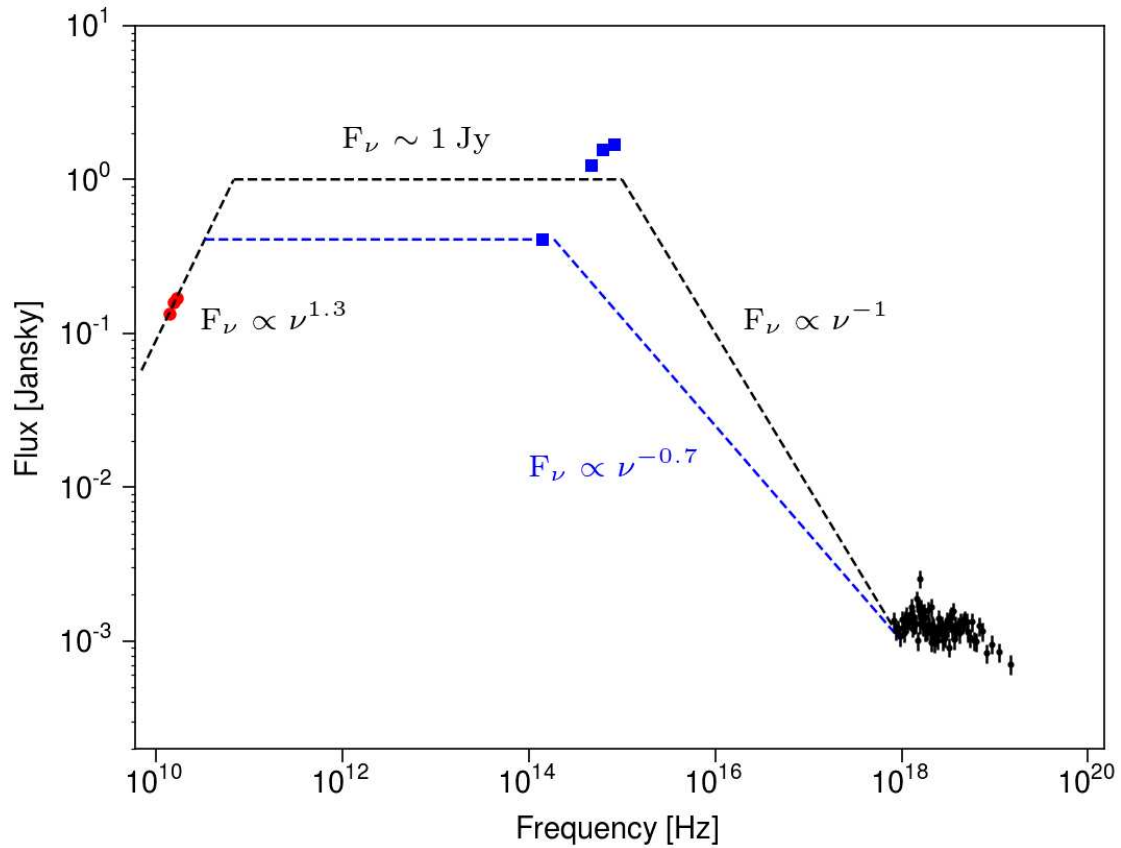


Fig. 4. Spectral energy distribution of the excess emission before the decay event. Fluxes plotted are for the radio (red circles), optical & infrared (blue squares), and x-ray (black crosses) observations (20). We present approximate spectral slopes (dashed lines connecting different energy regimes) as a rough guide to the slopes of apparent spectral breaks.

Supplementary Materials:

Materials and Methods

Figures S1-S3

Table S1

References (30-42)